ACS APPLIED MATERIALS & INTERFACES

Research Article

www.acsami.org

Optical Properties of Nanoporous Germanium Thin Films

Daniela Cavalcoli,*[,†] Giuliana Impellizzeri,[‡] Lucia Romano,[‡] Maria Miritello,[‡] Maria Grazia Grimaldi,[‡] and Beatrice Fraboni[†]

[†]Dipartimento di Fisica e Astronomia, Università di Bologna, Viale Berti Pichat 6/2, 40127 Bologna, Italy

[‡]CNR-IMM MATIS and Dipartimento di Fisica e Astronomia, Università di Catania,Via S. Sofia 64, 95123 Catania, Italy

Supporting Information

ABSTRACT: In the present article we report enhanced light absorption, tunable size-dependent blue shift, and efficient electron−hole pairs generation in Ge nanoporous films (np-Ge) grown on Si. The Ge films are grown by sputtering and molecular beam epitaxy; subsequently, the nanoporous structure is obtained by Ge+ self-implantation. We show, by surface photovoltage spectroscopy measurements, blue shift of the optical energy gap and strong signal enhancement effects in the np-Ge films. The blue shift is related to quantum confinement effects at the wall separating the pore in the structure, the signal enhancement to multiple light-scattering events, which result in enhanced absorption. All these characteristics are highly stable with time. These findings demonstrate that nanoporous Ge films can be very promising for photovoltaic applications.

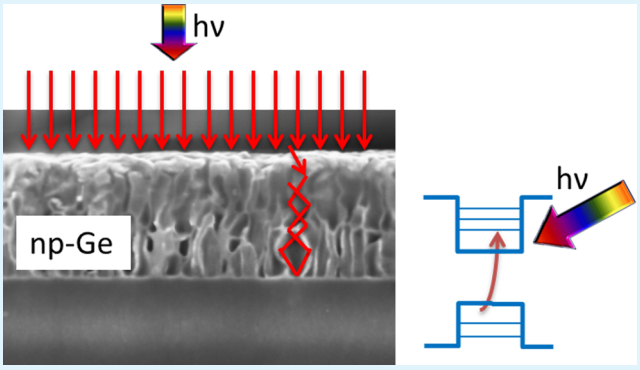

KEYWORDS: *quantum confinement, light trapping, surface photovoltage, nanoporous germanium, photovoltaic applications, ion implantation*

1. INTRODUCTION

Photovoltaic technology allows efficient conversion of solar energy into electrical power. In recent decades a very large amount of research has been done aiming to reduce the production prize and increase the efficiency of this technology. Thin film solar cells from several semiconductors can help reach the first goal, as they are usually obtained with low material usage and relatively low deposition temperatures; however, their energy conversion efficiency is still substantially lower than the one of crystalline semiconductors.[1] The following important issues can be effective to enhance the photovoltaic conversion efficiency: (1) improvement of sunlight absorption; (2) use of a tunable band gap material to optimize the matching with the solar spectrum; (3) reduction of parasitic absorption; (4) enhancement of minority carrier lifetime, that is, reduction of free carrier recombination. The present article deals with the first two issues, showing that nanoporous Ge thin film can efficiently address these two points.

Harvesting solar radiation is a fundamental issue to enhance light absorption. Efficient photon management and light trapping are mandatory to increase the amount of absorbed photons, and thus the photocurrent and efficiency of the cells. Several light management strategies have been considered so far to increase the fraction of light efficiently absorbed by the solar cell, like engineering plasmonic nanoparticles and gratings, resonant dielectric and photonic crystals, or implementing light scattering and wave interference in two-dimensional random media,[2] or in high refraction index nanostructures.[3,4] Among the different strategies recently proposed for photon management, one of the most interesting is the combination of efficient light trapping due to coherent optical effects with broad-band/wide-angle properties due to disorder.[2] Light propagation in a disordered structure is dominated by multiple scattering events and can be described in terms of a diffusive type of transport. In addition, interference phenomena can induce a slowing down of the light, increasing the probability of light−matter interaction. Interference could lead to weak or strong (Anderson) localization, where diffusion is decreased or completely halted. It has been demonstrated that a two-dimensional random film of finite thickness can lead to a large broad-band absorption enhancement,[2] but no direct observation of this phenomena in a three-dimensional system has been reported until now.[5,6]

Efficient solar cell conversion can be achieved if optical absorption and photogenerated charge-carrier transport are both optimized. The first issue is obtained if optimum matching between the solar spectrum and absorption edge is achieved, that is, if a material with tunable energy gap is employed for the cell. Tunable optical properties and even multiple exciton

Received: March 10, 2015
Accepted: July 16, 2015
Published: July 16, 2015

DOI: 10.1021/acsami.5b02089
ACS Appl. Mater. Interfaces 2015, 7, 16992−16998

Deposition	Scheme	Fluence-annealing (Ge+/cm^2)	Ge thickness (nm)	SPV signal
FILM, MBE		0	200	No
		1× 10 ^{16}	200	Yes
		2× 10 ^{16}	200	Yes
FILM, Sputter		2× 10 ^{16} + 500°C	200	Yes
		0	200, 400	No
		2× 10 ^{16}	200, 400	yes
BULK	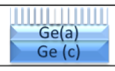	1× 10 ^{16}	375×10^3	yes

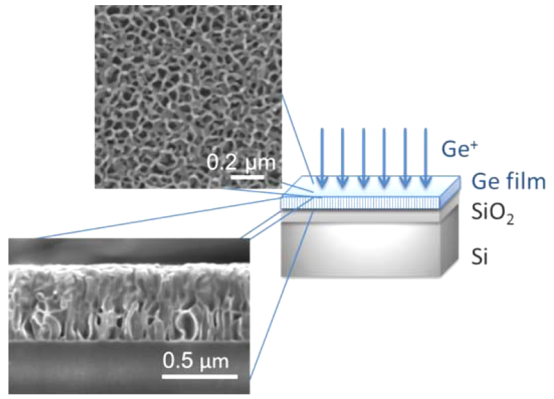

Figure 1. Deposition and implantation conditions and sketch of the implanted nanoporous Ge film structure.

generation can be achieved in semiconductor nanostructures due to quantum confinement effects through accurate control of shape, size, and surface properties. To achieve this target, different systems have been investigated, like quantum wells, wires, and dots.[7,8]

The second issue is still far from being completely achieved, as the quantum dots (QDs) are often embedded in a matrix with poor electrical-transport properties; thus, QD cell efficiency needs to be further improved. Recently, size-dependent energy band gap has been observed in ordered germanium nanoporous layers.[9] These structures present enormous advantages with respect to QDs embedded in a host matrix or quantum wires, for the interconnections between the nanosized objects which led to increased electrical transport.

Germanium has a number of characteristics that make it suitable for applications in solar energy conversion and electronics. It has a small band gap (0.67 eV), very high absorption coefficient, and refraction index in the portion of the electromagnetic radiation spectrum of the sunlight (4−4.5).[10] Moreover, quantum confinement effects can be activated at larger sizes with respect to Si due to the larger Bohr radius (24.3 vs 4.9 nm).[11]

In the present article we report on enhanced light-trapping and quantum confinement effects in disordered nanoporous Ge layers obtained by ion implantation. Several Ge films, obtained with different deposition conditions, and thus with different structural properties, have been investigated to analyze the effect of the structure on the optical properties. A strong increase of the photogenerated electron hole pairs for increasing the surface-to-volume ratio was observed by surface photovoltage (SPV) spectroscopy analyses. This behavior is a consequence of enhanced light trapping due to multiple scattering and/or strong/weak localization, as nanoporous Ge is a disordered structure. SPV spectroscopy also revealed a blue shift of the energy band gap for decreasing the dimensions of the pore wall thickness, due to quantum confinement effects. The SPV signal intensity is related to the number of photogenerated electron hole pairs, while its spectral dependence is related to the energy band gap. Thus, by measuring the SPV signal, we can obtain direct information on the capability of the system to convert light, while by analyzing the spectra, we obtain information on the tunability of the optical properties. Structural and morphological analyses were also performed to investigate the nanoporous samples. Therefore, the investigated nanoporous Ge film shows excellent properties for photovoltaic applications.

2. EXPERIMENTAL SECTION

Different sample sets of nanoporous Ge (np-Ge) were prepared and examined: two different np-Ge films [grown by molecular beam epitaxy (MBE) and sputtering] have been compared with np-Ge bulk samples. The thin film sample geometry and the deposition conditions are summarized in Figure 1. The formation of nanostructured porous Ge was reported to occur during implantation of Ge at room temperature (RT) with several heavy ions.[12−14] The resulting in-depth damage distribution consists of a porous amorphized Ge layer lying on a continuous amorphous layer. At the threshold fluence of 5×10^{15} cm^{-2} the 300 keV Ge$^+$ ion irradiated Ge substrate transforms into a porous amorphous structure, and in spite of the relatively low fluence, an enormous increase in surface area and a vertical expansion of the original Ge substrate occur, with a columnar structure of the porous layer. With a view on low-cost applications, it is particularly appealing to use thin films instead of bulk materials, which are expensive and not flexible.[12,13]

The first set of samples (film, MBE) is made of 200-nm-thick Ge layers, prepared by MBE on 500-nm-thick SiO_2 film thermally grown on Si substrates. During the depositions the substrate temperature was kept at 400 °C; at this growth temperature, the structure became polycrystalline.[14] The samples were then implanted with different Ge$^+$ fluences (1×10^{16} and 2×10^{16} Ge$^+$/cm^{-2}) at 300 keV to produce porous amorphous films. Some implanted samples were annealed in a conventional furnace at 500 °C for 1 h, in a N_2 atmosphere.

The second set (film, sputtering) is made of Ge layers 200- and 400-nm-thick, deposited at room temperature by dc-magnetron sputtering on a 1-μm-thick SiO_2 layer thermally grown on Si substrates. Because of the low deposition temperature, the film became amorphous. The samples were implanted at 2×10^{16} Ge$^+$/cm^2 at 300 keV, at RT to produce porous amorphous films.[12]

For comparison, the third set (bulk) is made of nanoporous bulk Ge samples, obtained by ion implantation (1×10^{16} cm^{-2}, 300 keV Ge+ at room temperature) of Ge Czochralski (100) crystals, 375-μm-thick, n-type (Sb-doped, resistivity higher than 40 Ω-cm). A porous amorphous layer, lying on a continuous amorphous layer, is obtained on top of crystalline bulk Ge. Further details and characterization studies of bulk nanoporous samples have been published elsewhere.[13−16]

Another set of samples has been prepared for study of the possible effect of ion-induced damage in the samples, whose characteristics are reported in the Supporting Information.

Sample morphology was investigated by scanning electron microscopy (SEM) with a field-emission Zeiss Supra 25. Surface Photovoltage spectroscopy was performed at room temperature by means of a custom-made apparatus based on a SPEX 500 M monochromator. The system allows for the measurement of the surface photovoltage (SPV) signal in a wide spectral range (λ ranging from 300 to 2000 nm) by the use of different gratings and light sources (quartz-tungsten-halogen and xenon lamps). More detailed information on the experimental setup can be found elsewhere.[17]

DOI: 10.1021/acsami.5b02089
ACS Appl. Mater. Interfaces 2015, 7, 16992−16998

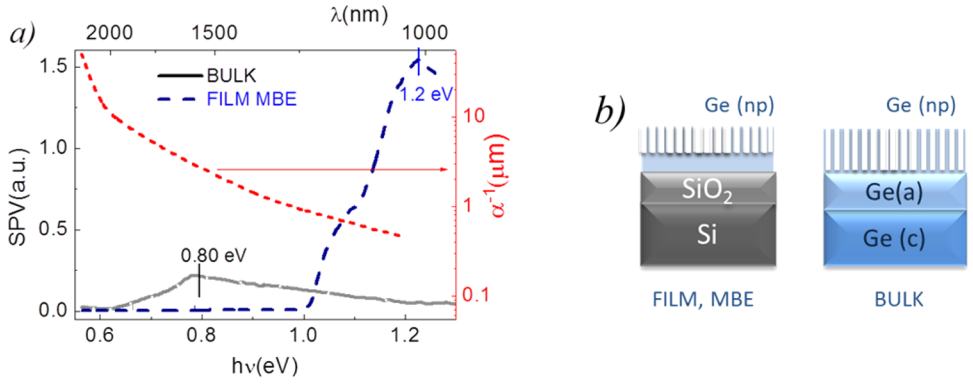

Figure 2. (a) SPV spectra of np-Ge film deposited by MBE (FILM, MBE) compared with BULK np-Ge. The estimated penetration depth α^{-1} of the impinging photons is also reported (right axis) as evaluated by Dash et al.[19] Reprinted with permission from ref 19. Copyright 1955 American Physical Society. (b) Sketch of the sample geometry.

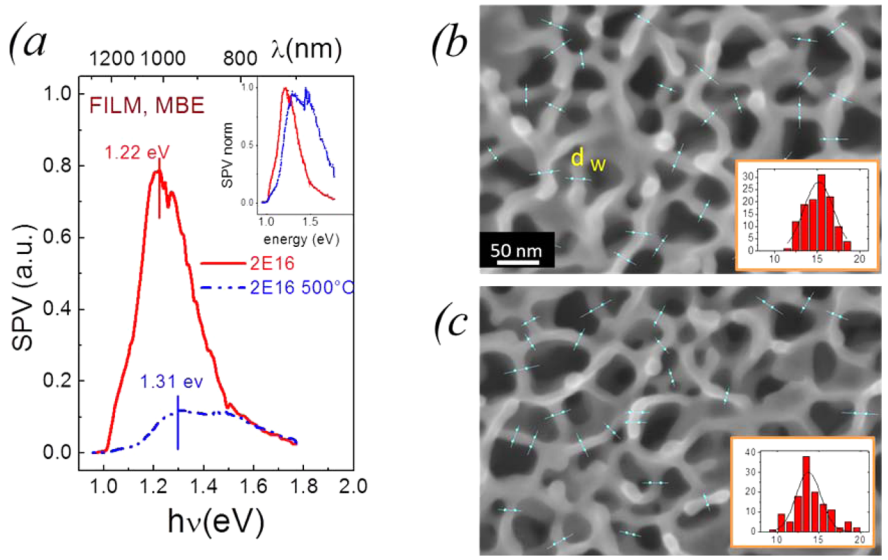

Figure 3. (a) Surface photovoltage spectra of the film, MBE np-Ge layers implanted at 2×10^{16} (labeled 2E16 in the figure) before and after 500 °C annealing. Normalized SPV spectra are reported in the inset for comparison. (b, c) SEM plan view of (b) as implanted and (c) 500 °C annealed samples. Same examples of data lines used for statistical sampling are reported in light blue. Scale marker is the same (50 nm); histogram abscissa has unit of measure of nm.

Surface photovoltage spectroscopy is a valuable tool for the investigation of optoelectronic properties of semiconductors, thin films, and heterostructures. The method has been extensively reviewed in ref 18. The SPV signal is defined as the illumination-induced variation of the semiconductor surface potential. The signal, capacitively picked up by a semitransparent electrode, goes through a high impedance field-effect transistor preamplifier and is measured by a lock-in amplifier. A suitable cutoff filter is used to get rid of higher order spectral diffraction lines. The spectral resolution of the system is better than 2 nm, which results, in the spectral range used in this study, in energy resolution ranging from 0.4 to 1.6 meV. Nevertheless, because of the unavoidable indetermination associated with the identification of the main electronic transition in the SPV spectra, an error bar of 0.01 eV is associated with the energy values presented here. SPV spectra are usually showed by plotting the SPV signal divided by the photon flux (normalized spectra) as a function of photon energy. The most relevant peak in a SPV spectrum is usually related to band-to-band electronic transitions.[18] As the signal comes from a surface-related phenomenon, a usually intense SPV signal can be measured in nanostructures where the surface-to-volume ratio is very high.

3. RESULTS AND DISCUSSION

Very reproducible and stable SPV spectra were observed in all the implanted nanoporous Ge films, while in reference as-deposited, not-implanted Ge films obtained by MBE and sputtering measurable SPV signals were undetectable in the whole spectral range explored. The lack of signal in the as-deposited films can be due to strong recombination of the photogenerated carriers at the SiO_2−Ge interface.

Instead, in the np-Ge film, thanks to their high surface-to-volume ratio that enhances the probability of electron−hole pair photogeneration, the loss of carriers at the interface is completely balanced by the large amount of carriers photogenerated at the surface. On the basis of this evidence, we can hypothesize that strong light-trapping effects further enhance light absorption and thus the SPV signal in the nanoporous layers.

Figure 2a shows the normalized SPV spectrum of MBE-grown np-Ge thin film (film, MBE) obtained by ion implantation with a fluence of 2×10^{16} Ge^+/cm^2 (blue dashed line). The spectrum is compared with the one obtained on np-Ge bulk samples obtained at the same fluence (dark solid line).

DOI: 10.1021/acsami.5b02089
ACS Appl. Mater. Interfaces 2015, 7, 16992−16998

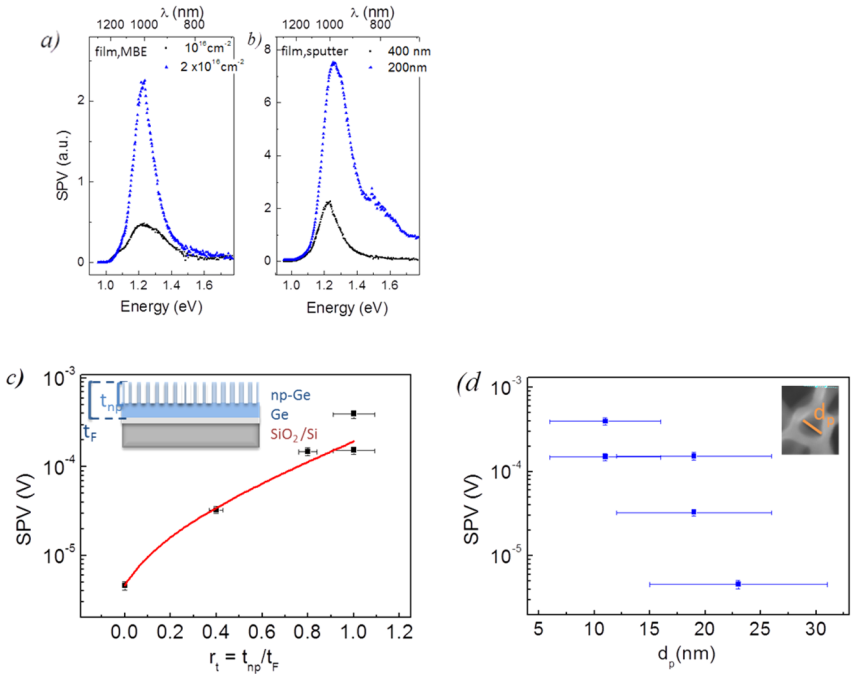

Figure 4. SPV spectra of np-Ge films deposited by MBE and implanted at different fluences (a) and deposited by sputtering with different thicknesses implanted at the same fluence (2×10^{16} cm^{-2}) (b). SPV maximum signal is plotted versus the ratio r_t between the nanoporous layer thickness t_{np} and the whole film thickness t_F. The red line is a guide for the eye (c) and as a function of the average pore diameter d_p (d). The morphological parameters are defined in the insets.

The sample sketch is also inserted (Figure 2b). The spectra contain features (slope variations) that are related to photo-induced electronic transitions. The main features (maxima) of the spectra must be related to band-to-band electronic transitions; therefore, the two maxima correspond to the optical energy gap. While the energy gap of bulk np-Ge compares well with the direct band gap of crystalline Ge (0.80 eV), a significant blue shift of the energy gap of the np-Ge film (1.20 eV) is observed. In Figure 2 the spectral dependence of the light penetration depth (α^{-1}) is also reported (red short-dashed line).[19] Although the absorption length here plotted refers to crystalline Ge, whose optical property significantly differs from the present Ge films, we used this value to obtain an estimate of the order of magnitude of α^{-1}. The maximum of the np-Ge thin film spectrum occurs at 1.2 eV; at this energy α^{-1} is well below 1 μm, indicating that carrier generation and separation occurs within the np-Ge film. The spectra in Figure 2a represent the signal divided by the photon flux and have been obtained at the same illumination condition, so the intensities of the two spectra can be compared. It must be noted that the np-Ge film shows a SPV signal whose intensity is 1 order of magnitude higher than the signal of the bulk np-Ge sample. This effect will be explained later on in the article. In Figure 3a the SPV spectra of MBE-grown np-Ge thin films obtained by ion implantation with a fluence of 2×10^{16} Ge$^+$/cm^{-2} before and after annealing treatment at 500 °C are compared. The two measurements have been carried out at the same illumination condition. A significant blue shift of the energy gap, moving from 1.22 to 1.31 eV, and a strong reduction of the signal intensity after annealing are evident from such a comparison. To understand the first effect, SEM analyses of the two samples have been compared; the results are presented in Figure 3b,c. Pores separated by walls whose dimensions are in the nanometer range make up the porous structure. A careful analysis of the wall size (d_W) measured on several micrographs at different magnifications resulted in the d_W distributions plotted in the insets of Figure 3b,c. While d_W ranges from 12 to 17 nm in the np-Ge as an implanted sample, it ranges from 9 to 15 in the annealed sample.

If we assume a possible quantum confinement mechanism of free electrons inside the walls, according to what is proposed by Armatas et al.,[9] the reduction of the average wall size upon annealing can explain the observed blue shift. As a matter of fact, as SPV allows for the detection of electronic transitions, the maximum in the SPV spectra corresponds to transitions at confined electronic states within the structure. In addition, the d_W distribution broadens after annealing, as well as the SPV peak (Figure 3a, inset). The strong reduction of the SPV signal intensity after annealing has been observed also for the samples implanted at 1×10^{16} Ge$^+$/cm^2. This can be related to Si−Ge intermixing at the interface and/or to annealing-induced GeO_2 formation at the sample surface.[20,21] A Si−Ge phase has been observed in the literature at annealing temperatures close to 500 °C[22,25] likely due to the possible diffusion of Si from the SiO_2 substrate. The formation of a disturbed interface between Ge and SiO_2 can reduce the SPV signal due to enhanced recombination.

Figure 4 a,b shows SPV spectra of MBE and sputter-deposited np-Ge film, respectively, obtained at different fluences and thicknesses. The spectra can be compared as they have been measured at the same illumination conditions. The maxima of the spectra appear at energy values close to 1.2 eV for all the spectra, but remarkable differences can be noted in the signal intensity of the different samples. In MBE-grown samples the signal intensity increases for an increase of the Ge$^+$ fluence. As the vertical expansion of the implanted layer increases almost linearly with fluence,[15] we can infer that an increase in the nanoporous layer thickness causes an increase in

DOI: 10.1021/acsami.5b02089
ACS Appl. Mater. Interfaces 2015, 7, 16992−16998

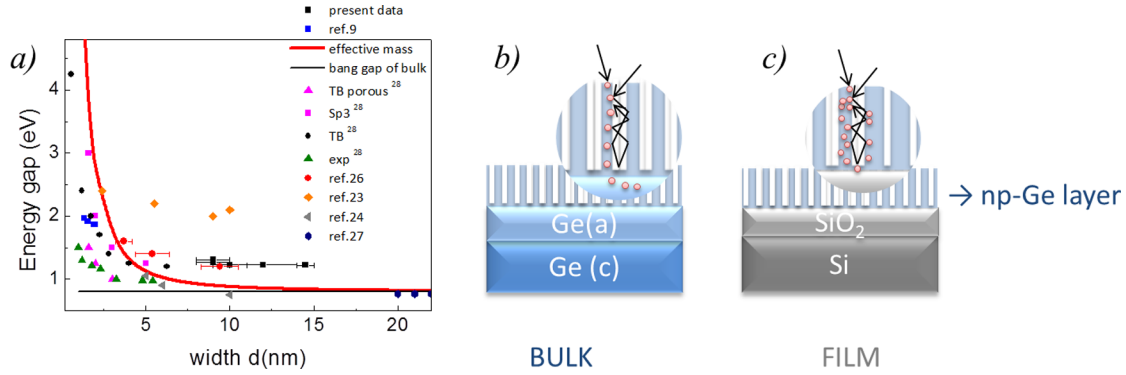

Figure 5. (a) Measured energy gap values (square dots with error bars) plotted as a function of the average wall size d compared with experimental literature data,[9,23,24,26,27] theoretical literature data,[28] and effective mass model (solid red line). Data reprinted with permission from ref 9, Copyright 2010 American Chemical Society; ref 23, Copyright 2013 American Chemical Society; ref 24, Copyright 2014 American Institute of Physics; ref 26, Copyright 2014 American Chemical Society; ref 27, Copyright 2012 Elsevier; ref 28, Copyright 2013 American Institute of Physics. Sketch of the np-Ge film (b) and bulk (c) samples. Light trapping is sketched as a dark line and free carrier generation as red dots.

the SPV signal. Intriguing, the sputter-deposited samples show the opposite result: here, both samples have been implanted with the same fluence (2×10^{16} Ge^+/cm^2), the sample with lower film thickness showing the maximum signal. To understand this behavior, we analyzed the effect of morphological parameters on the SPV signal intensity. In particular, we correlated the maximum SPV signal with the average pore diameter d_P, and with the ratio r_t between the np-layer thickness t_{np} and the whole film thickness t_F. All the morphological parameters were obtained by measuring the film thicknesses of the porous layers by SEM and transmission electron microscopy.[12,14,15]

Figure 4c,d reports the absolute value of the maximum SPV signal, measured at the same illumination conditions for all the nanoporous samples, as a function of r_t and d_p, respectively. The schematics in the inset show the definition of the morphological parameters. It is worth noting that the SPV signal increases as a function of r_t, while it is almost independent of the pore diameter for d_p in the 10−30 nm range. The SPV maximum intensity is proportional to the amount of photogenerated and collected electron−hole pairs; thus, the increase of the SPV signal implies an increase of light trapping and charge separation. As r_t indicates the amount of the nanoporous layer over the whole film volume, the increase of the SPV vs r_t means that the larger the nanoporous fraction, the larger the light-trapping effect. Since the Ge-np layer obtained by sputtering with thickness of 200 nm, implanted at 2×10^{16} cm^{-2}, becomes almost completely nanoporous,[12,15] this sample has the highest surface-to-volume ratio and shows the highest SPV signal (see Figure 4b). In addition, the photogenerated electron−hole pairs are efficiently collected by this structure due to optimum quantum confinement, as in this case the whole film is nanoporous and its bottom surface corresponds to the Ge/SiO_2 interface that acts as a potential barrier for the charged carriers. It must also be mentioned that the high intensity of the SPV signal remains stable with time, as the spectra measured after 1 year do not show any variation (see Supporting Information). As the measurements are performed at ambient conditions, this means that water molecules and humidity have no influence on the optoelectronic properties of the samples. The independence of the SPV signal on the pore diameter (Figure 4d) can be related to the fact that both pore diameters and wall dimensions are significantly smaller than the photon wavelength λ (in our experiments λ ranges from 700 to 1300 nm); therefore, a Rayleigh-type scattering mechanism should apply in all the samples. It is possible to argue that larger nanostructures, with dimensions comparable with λ, could give rise to different scattering mechanisms and thus in this case a variation of the signal with the pore diameter could occur.

To better understand the blue shift observed by SPV on nanoporous Ge films, the values of the measured energy gap have been plotted as a function of the average wall sizes d_W of the samples measured by SEM micrographs (Figure 3b,c). The large error bars represent the standard variation of d_W distribution. These data are compared with published experimental results obtained for nanoporous Ge[9], Ge nanocrystals,[23,24,26] and theoretical and experimental data replotted from ref 28 as a function of the confinement dimension d. The dependence of the energy gap on d is also calculated by the effective mass model formula and plotted in Figure 5 as a solid line. The results show a quite large dispersion for several different reasons: first, the effective mass theory is an approximated model and, second, experimental data plotted here are measured by emission and absorption spectroscopies and refer to different nanostructures (ordered nanoporous structures, nanocrystals, and nanowires) embedded in different matrixes. Moreover, besides the different embedding medium which certainly plays a role,[22] the surface termination should affect the results, and in the present case we should assume the presence of a Ge−O termination layer at the surface of our structures.[29] Nevertheless, it is interesting to note the very good agreement of our experimental data with the results obtained by Muthuswamy et al.[26] on Ge nanocrystals by SPV.

Since the porous structure examined here has been obtained by Ge ion implantation, and it is well-known that ion implantation can induce different point defects; we checked the possible effect of ion-induced defects in the measured SPV spectra. Different implant conditions have been chosen to localize the ion-induced damage at the same depth in the structure as in np samples; these details are described in the Supporting Information. Figure S1 shows SPV spectra of ion-implanted samples specifically prepared to check this effect; the comparison shows that defect states induced by ion implantation result in a well-detectable band located around 1.60−1.67 eV. However, these bands of states are not present in the spectrum of the nanoporous Ge film. Therefore, we can

DOI: 10.1021/acsami.5b02089
ACS Appl. Mater. Interfaces 2015, 7, 16992−16998

conclude that the feature at 1.2 eV that we reveal in the nanoporous samples is not due to any defect in the substrate or at the substrate/Ge layer interface.

4. CONCLUSIONS

Quantum confinement and light-trapping effects in nanoporous Ge films obtained via ion self-implantation were assessed by surface photovoltage spectroscopy. Films deposited in different conditions, with different structural characteristics, show very similar optoelectronic properties.

A clear blue shift of the energy gap for decreasing the size of the walls separating the pore is observed. This blue shift is observed for confinement dimensions up to 14 nm, according to what has been found for colloidal nanocrystals[27] and consistently to large Ge Bohr radius.[11] It is important to note that a similar effect has not been observed in bulk nanoporous Ge samples. To explain this, we can refer to the sketch in Figure 5b,c. In bulk np-Ge samples the photogenerated free carriers are allowed to freely move from the nanoporous layer to the continuously connected Ge substrate, thus loosing confinement. In contrast, in np-Ge films the photogenerated carriers remain confined within the nanostructure as they will encounter a potential barrier at the interface with SiO_2 to reach the substrate. Besides quantum confinement, a strong increase in the SPV intensity has been observed in thin film np-Ge samples. This signal enhancement must be related to two different effects: light trapping within the pores and carrier confinement. The first effect causes absorption enhancement, which has already been reported for a two-dimensional random film of finite thickness,[2,5,6] but never reported until now for 3D systems. The second effect has already been observed in ordered germanium nanoporous materials,[9] and in Ge nanowires,[27] but never in nanoporous Ge films obtained by ion implantation.

Figure 5b,c shows a sketch representing the light−matter interaction in nanoporous bulk and film samples. Multiple light-scattering mechanisms occurring within the pores enhance the probability of electron−hole generation within the film. The photogenerated free carriers are confined within the structure and cannot leave the nanoporous layer, thus inducing a strong variation in the surface potential. This variation is just the surface photovoltage. The intense SPV signal detected in the present study is therefore due to the multiple light-scattering events that create a large amount of carriers that remain confined within the structure. In addition, the contrast between the refraction index of Ge and SiO_2 can also play a role, but it cannot be responsible by itself for the enhancement of the SPV signal, as unimplanted Ge films do not show any significant signal.

It is important to emphasize, in view of the possible application of the present structure in the photovoltaic field, that we have revealed not only enhanced light trapping by the nanoporous structure, which indicates a strong light absorption in the structure, but also very efficient photogeneration of free carrier, which is a key point to achieve very efficient photovoltaic devices. In addition, previous studies demonstrate that these porous Ge show enhanced conductivity and excellent transport properties.[13]

In conclusion, the observed nanoporous Ge layers can efficiently absorb sunlight and can generate free carriers that can easily circulate and thus could be collected generating a photocurrent. All these processes occur at tunable energies; thus, an optimum match with the solar spectrum can be achieved. To achieve a highly efficient solar cell, some issues must still be addressed, such as the realization of a suitable structure for free carrier separation; however, the present results demonstrate that this material shows excellent properties in view of photovoltaic applications.

■ ASSOCIATED CONTENT

Supporting Information

Sample description and SPV analyses of samples subjected to similar ion implantation conditions compared to the ones presented in this article, but without the nanoporous layer. This comparison allows us to control the role of ion-induced defects on the SPV spectra. In addition, we present SPV spectra showing the stability of the samples after 1 year of storage. The Supporting Information is available free of charge on the ACS Publications website at DOI: 10.1021/acsami.5b02089.

■ AUTHOR INFORMATION

Corresponding Author

*E-mail: Daniela.cavalcoli@unibo.it.

Notes

The authors declare no competing financial interest.

■ REFERENCES

(1) Green, M. A.; Emery, K.; Hishikawa, Y.; Warta, W.; Dunlop, E. D. Solar Cell Efficiency Tables (version 44). *Prog. Photovoltaics* **2014**, *22*, 701−710.

(2) Vynck, K.; Burresi, M.; Riboli, F.; Wiersma, D. S. Photon Management in Two-Dimensional Disordered Media. *Nat. Mater.* **2012**, *11*, 1017−1022.

(3) Brongersma, M. L.; Cui, Y.; Fan, S. Light Management for Photovoltaics Using High-index Nanostructures. *Nat. Mater.* **2014**, *13*, 451−460.

(4) Cao, L.; White, J. S.; Park, J.-S.; Schuller, J. A.; Clemens, B. M.; Brongersma, M. L. Engineering Light Absorption in Semiconductor Nanowire Devices. *Nat. Mater.* **2009**, *8*, 643−647.

(5) Wiersma, D. S. Disordered Photonics. *Nat. Photonics* **2013**, *7*, 188−196.

(6) Burresi, M.; Wiersma, D. S. Complex Photonic Structures for Energy Efficiency. *EPJ Web Conf.* **2013**, *54*, 01016−01031.

(7) Priolo, F.; Gregorkiewicz, T.; Galli, M.; Krauss, T. F. Silicon Nanostructures for Photonics and Photovoltaics. *Nat. Nanotechnol.* **2014**, *9*, 19−32.

(8) Nozik, A. J.; Beard, M. C.; Luther, J. M.; Law, M.; Ellingson, R. J.; Johnson, J. C. Semiconductor Quantum Dots and Quantum Dot Arrays and Applications of Multiple Exciton Generation to Third-Generation Photovoltaic Solar Cells. *Chem. Rev.* **2010**, *110*, 6873−6890.

(9) Armatas, G. S.; Kanatzidis, M. G. Size Dependence in Hexagonal Mesoporous Germanium: Pore Wall Thickness versus Energy Gap and Photoluminescence. *Nano Lett.* **2010**, *10*, 3330−3336.

(10) Philipp, H. R.; Taft, E. A. Optical Constants of Germanium in the Region 1 to 10 eV. *Phys. Rev.* **1959**, *113*, 1002−1005.

(11) Maeda, Y.; Tsukamoto, N.; Yazawa, Y.; Kanemitsu, Y.; Masumoto, Y. Visible Photoluminescence of Ge Microcrystals Embedded in SiO2 Glassy Matrices. *Appl. Phys. Lett.* **1991**, *59*, 3168−3171.

(12) Romano, L.; Impellizzeri, G.; Tomasello, M. V.; Giannazzo, F.; Spinella, C.; Grimaldi, M. G. Nanostructuring in Ge by Self-ion Implantation. *J. Appl. Phys.* **2010**, *107*, 084314−084319.

(13) Impellizzeri, G.; Romano, L.; Fraboni, B.; Scavetta, E.; Ruffino, F.; Bongiorno, C.; Privitera, V.; Grimaldi, M. G. Nanoporous Ge Electrode as a Template for Nano-sized (< 5 nm) Au Aggregates. *Nanotechnology* **2012**, *23*, 395604−395610.

(14) Impellizzeri, G.; Romano, L.; Bosco, L.; Spinella, C.; Grimaldi, M. G. Nanoporosity Induced by Ion Implantation in Germanium Thin

DOI: 10.1021/acsami.5b02089
ACS Appl. Mater. Interfaces 2015, 7, 16992−16998

Films Grown by Molecular Beam Epitaxy. *Appl. Phys. Express* **2012**, *5*, 035201−035204.
(15) Romano, L.; Impellizzeri, G.; Bosco, L.; Ruffino, F.; Miritello, M.; Grimaldi, M. G. Nanoporosity Induced by Ion Implantation in Deposited Amorphous Ge Thin Films. *J. Appl. Phys.* **2012**, *111*, 113515−113510.
(16) Cavalcoli, D.; Fraboni, B.; Impellizzeri, G.; Romano, L.; Scavetta, E.; Grimaldi, M. G. Optoelectronic Properties of Nanoporous Ge Layers Investigated by Surface Photovoltage Spectroscopy. *Microporous Mesoporous Mater.* **2014**, *196*, 175−178.
(17) Cavalcoli, D.; Fraboni, B.; Cavallini, A. Surface and Defect States in Semiconductors Investigated by Surface Photovoltage. *Semicond. Semimetals: Defects in Semiconductors* **2015**, *91*, 251−278.
(18) Kronik, L.; Shapira, Y. Surface Photovoltage Phenomena: Theory, Experiment, and Applications. *Surf. Sci. Rep.* **1999**, *37*, 1−206.
(19) Dash, W. C.; Newman, R. Intrinsic Optical Absorption in Single-Crystal Germanium and Silicon at 77 K and 300 K. *Phys. Rev.* **1955**, *99*, 1151−1155.
(20) Romano, L.; Impellizzeri, G.; Grimaldi, M. G. Influence of Microstructure on Voids Nucleation in Nanoporous Ge. *Mater. Lett.* **2013**, *96*, 74.
(21) Hashemi, F. S. M.; Thombare, S.; Fontcuberta i Morral, A.; Brongersma, M. L.; McIntyre, P. C. Effects of Surface Oxide Formation on Germanium Nanowire Band-edge Photoluminescence. *Appl. Phys. Lett.* **2013**, *102*, 251122−251126.
(22) Ray, S. K.; Maikap, S.; Banerjee, W.; Das, S. Nanocrystals for Silicon-Based Light-Emitting and Memory devices. *J. Phys. D: Appl. Phys.* **2013**, *46*, 153001−153031.
(23) Wheeler, L. M.; Levij, L. M.; Kortshagen, U. R. Tunable Band Gap Emission and Surface Passivation of Germanium Nanocrystals Synthesized in the Gas Phase. *J. Phys. Chem. Lett.* **2013**, *4*, 3392−3396.
(24) Singha, R. K.; Manna, S.; Das, S.; Dhar, A.; Ray, S. K. Room Temperature Infrared Photoresponse of Self-Assembled Ge/Si (001) Quantum Dots Grown by Molecular Beam Epitaxy. *Appl. Phys. Lett.* **2010**, *96*, 233113−233117.
(25) Ding, L.; Lim, A. E-J; Liow, J. T.-Y.; Yu, M. B.; Lo, G.-Q. Dependences of Photoluminescence from P Implanted Epitaxial Ge. *Opt. Express* **2012**, *20*, 8228−8239.
(26) Muthuswamy, E.; Zhao, J.; Tabatabaei, K.; Amador, M. M.; Holmes, M. A.; Osterloh, F. E.; Kauzlarich, S. M. Thiol-Capped Germanium Nanocrystals: Preparation and Evidence for Quantum Size Effects. *Chem. Mater.* **2014**, *26*, 2138−2146.
(27) Miranda, A.; Trejo, A.; Canadell, E.; Rurali, R.; Cruz-Irisson, M. Interconnection Effects on the Electronic and Optical Properties of Ge Nanostructures: A Semi-Empirical approach. *Phys. E (Amsterdam, Neth.)* **2012**, *44*, 1230−1235.
(28) Parola, S.; Quesnel, E.; Muffato, V.; Bartringer, J.; Slaoui, A. Influence of the Embedding Matrix on Optical Properties of Ge Nanocrystals-based Nanocomposite. *J. Appl. Phys.* **2013**, *113*, 05351−053520.
(29) Holman, Z. C.; Kortshagen, U. R. Absolute absorption Cross Sections of Ligand-Free Colloidal Germanium Nanocrystals. *Appl. Phys. Lett.* **2012**, *100*, 133108−133112.

DOI: 10.1021/acsami.5b02089
ACS Appl. Mater. Interfaces 2015, 7, 16992−16998